RESEARCH ARTICLE

Recent Advances on Drug Delivery Systems for Viral Infections

Curcumin/Fusidic Acid Bitherapy Loaded Mixed Micellar Nanogel for Acne Vulgaris Treatment: *In Vitro* and *In Vivo* Studies

Raghda Abdel-monem[1] · Eman S. El-leithy[1,2] · Ahmed Adel Alaa-Eldin[3] · Rania S. Abdel-Rashid[1]

Abstract

The combination of herbal drugs with a topical antibacterial for managing a chronic disease like acne vulgaris has emerged lately to settle side effects and bacterial multidrug resistance. Mixed micelles (MMs) incorporated into nanogel were explored for hybrid delivery of curcumin (Cur) and fusidic acid (FA) combination presenting a multi-strategic treatment. Curcumin-fusidic acid–loaded mixed micelles (Cur-FA-MMs) were assessed for size, surface charge, compatibility, *in vitro* release, and encapsulation. The selected formula was further loaded into nanogel and investigated for viscosity, *ex vivo* permeation, and *in vivo* potential. Cur-FA-MMs exhibited uniform nanosized spherical morphology, and negative surface charge affording high encapsulation for both drugs with a biphasic *in vitro* release over a period of 48h and good colloidal stability. The attained Cur-FA-MM-loaded nanogel had optimum viscosity with remarkable permeation coefficient values nearly 2-fold that related to plain nanogel. The pharmacodynamic effect of Cur on FA was pronounced by the significant improvement of the skin's degree of inflammation, epidermal hypertrophy, and congestion in animals treated with Cur-FA-MM-loaded nanogel. In conclusion, micellar nanogel could enable the *progressive* effect of Cur (an antioxidant with reported antibiotic activity) on FA (antibiotic) and decrease the risk of emerging antibiotic resistance by enhancing the solubility and permeation of Cur.

Keywords acne vulgaris · combination therapy · curcumin · fusidic acid · mixed micelles · nanogel

Introduction

Acne vulgaris is a distinctive chronic skin infection that affects face, neck, and upper part of chest exhibiting lesions which resulted from excessive sebum production, altered keratinization, and inflammation of pilosebaceous follicular units as well as colonization of bacterial biofilm [1, 2]. It has been known that acne affects about 80% of individuals through their lives accompanied with drastic impacts on their social and psychological life, loss of self-confidence, anxiety, and depression [3, 4]. Genetics, hormonal disturbance, dietary factors, cosmetics, stress, and drawbacks of certain medications are all important factors that can prompt acne vulgaris [5].

Based on level of acne lesions and severity of inflammation, different types of therapies are selected [6]. Topical and oral medical treatments such as antibiotics and retinoids are the most popular treatments used for mild and moderate acne [7]. However, those remedies have demonstrated some disadvantages which bother patients, as GIT upset, ulcerative colitis, depression, teratogenicity, extreme dryness, skin peeling, erythema, and dermatitis [8–10].

Fusidic acid (*FA*) is a bacteriostatic agent with a steroidal chemical nature, recommended for treating primary and secondary skin diseases and ocular infections [11]. FA is characterized by its narrow spectrum bacteriostatic activity (Gram-positive bacteria) whereas many infections triggered by multi-resistance species of bacteria can highly hinder its pharmacological activity. It is available in oral,

✉ Raghda Abdel-monem
   raghda_ali@pharm.helwan.edu.eg;
   abdelmoneumraghda@hotmail.com

   Eman S. El-leithy
   esaddar@msa.edu.eg

   Ahmed Adel Alaa-Eldin
   aam34@fayoum.edu.eg

   Rania S. Abdel-Rashid
   sansoova@yahoo.com; rania.safa@pharm.helwan.edu.eg

1   Department of Pharmaceutics and Industrial Pharmacy,
    Faculty of Pharmacy, Helwan University, Cairo 11795, Egypt

2   Department of Pharmaceutics and Industrial Pharmacy,
    Faculty of Pharmacy, October University for Modern
    Sciences and Arts (MSA), Cairo, Egypt

3   Faculty of Pharmacy, Fayoum University, Fayoum, Egypt

parenteral, and topical dosage forms, and each is associated with numerous hazards and hitches [12]. Recognizing the severe drawbacks accompanied with commercially available acne vulgaris therapy including FA different topical dosage forms, it has been becoming increasingly important to focus on new strategies to limit these side effects. The combination of herbal drugs with topical antibacterial treatment for the efficient and safe management of acne vulgaris has been investigated lately in order to overcome side effects and multidrug resistance reaching the optimum therapeutic regimen [13–16].

Herbal remedies gained their popularity owing to their various advantages including safety, abundancy in nature, few side effects, better therapeutic action, more patient compilance, and cost-effectiveness [17]. They can be utilized alone or in combination with other drugs for *better* effect, declining the side effects of other drugs. Among herbal remedies, curcumin (*Cur*) is considered the most potent medicinal plant, widely used owing to its broad pharmacological actions like antioxidant, anti-inflammatory, antimicrobial, anticancer, and immunomodulatory activity which are all related to its unique structure [18–20].

Referring to the previously mentioned activities, it can be used for treatment of several skin conditions such as acne vulgaris, atopic dermatitis, eczema, and psoriasis with few adverse effects [21]. Moreover, Cur safety has been proved in animal studies as well as clinical trials [22]. Additionally, Cur displayed worthy accessibilty and bioactivity of combination therapy mainly after merging in novel preparations making it tolerable therapeutic agent for healing of topical skin disorders [21].

Different nanosized-based formulations were developed as effective alternative drug delivery to conventional topical skin treatments providing high drug loading capacity, targeting effect, improving drug permeability, and removing characteristic signs of acne vulgaris [6].

Mixed micelles (*MMs*) have raised distinct interest as nano-sized carriers due to their exceptional physical and chemical characteristics. The benefits of those carriers especially in antibacterial preparations comprise high loading capacity with good solubilization, and extended drug release, targeting drug delivery to the infection site with abundant stability [23]. MMs also improved cellular internalization attaining hyper sensitization towards multidrug-resistant cells with minimum systemic side effects than of the individual components [24]. Moreover, the utilized surfactants perform as permeation enhancer and can enhance drugs flux by decaying skin stratum corneum structure [25].

The aim of this investigation was to explore the potential of lecithin–Tween 80 mixed micellar system incorporating Cur-FA combined bitherapy, to overcome drawbacks and limitations associated with topical FA. The MMs were developed using thin-film dispersion method and the optimized mixed micelle dispersion was then loaded into nanogel which their physical assets, viscosity, and *ex vivo* permeation were studied. An *in vivo* model was conducted to assess anti acne activity for curcumin-fusidic acid–loaded mixed micelles (Cur-FA-MM)-loaded nanogel compared to conventional free drug–loaded nanogels.

Materials and Methods

Materials

Cur was obtained via Sigma-Aldrich Co (St. Louis, MO, USA). FA was kindly gifted by EVA pharmaceuticals, Giza, Egypt. Tween 80 was supplied by MP Biomedicals (Santa Ana, CA, USA). Lecithin was gifted from NODCAR, Egypt. Sodium hydroxide and Potassium dihydrogen orthophosphate were bought from El-Nasr Pharmaceutical Chemicals Co., Egypt. Methanol and double-distilled water were used throughout the study. Carbopol 934 and Triethanolamine (HPLC grade) were procured from El- Gomhouria Chemicals Pharmaceutical Company, Egypt.

Methods

Validation of Spectrophotometric Method Used for Determination of Cur and FA Mixture

The study was based on the simultaneous delivery of Cur and FA from one nanocarrier system; therefore, it was a must to ensure absence of overlapping, accredit validity, and precision of the method used for measurement of drug concentrations. Using UV-VIS spectrophotometer (JASCO V-530 double beam), individual solutions of known concentrations of Cur and FA as well as a mixture of both drugs were scanned at a UV range 200–400nm. After determination of the characteristic UV wavelength for each drug, calibration curves were constructed for each one. Validation of the method established was investigated by different studies like repeatability and intermediate precision. In repeatability (intra-day), the amounts of Cur and FA in a mixture were estimated on the same day three times at 2-h intervals. In intermediate precision (inter-day) study, the amounts of drugs in mixture were estimated on three successive days.

Fabrication of MMs Loaded with Combined Cur/FA

MMs including both Cur and FA were formulated by a thin-film dispersion technique [26]. Accurately weighed amounts of Cur, FA, lecithin, and Tween 80 were solubilized into blend of methanol and dichloromethane at ratio (3:7;v/v) then under reduced pressure at 40°C at 200 rpm using rotary evaporator (IKA, HBIO basic, RV10B

S99, Deutschland, Germany); the obtained mixture was converted into a thin film. The film was then subjected to three steps; firstly, the film was allowed to dry overnight in room temperature to remove the excess methanol. Secondly, 5ml distilled water was added for film hydration followed by another 5ml for washing off the remaining [27]. Then, the film was dispersed via water bath sonicator with frequency 30 kHz for 7 min leading to production of micellar dispersion. The dispersion was then subjected to centrifugation at 12,000 rpm for 15min and the supernatant was collected containing the Cur-FA-MMs [26]. The effect of different concentrations of FA, Tween 80, and lecithin was studied at constant concentration of Cur as presented in Table I.

Characterization of Prepared MMs

Micelle Size, PDI, Surface Charge The size is a vital clue in the assessment of nanocarrier delivery systems. The mean size, polydispersity, and zeta potential of Cur-FA-MMs were detected by Zetasizer at an angle of 90° (Malvern Instruments, Malvern, UK) [28]. The samples were diluted using double-distilled water prior each measurement. All the tests were performed in triplicate at room temperature (25°C).

Efficiency of Encapsulation and Drug Loading The amounts of Cur and FA in Cur-FA-MMs encapsulated were quantified at 426 nm and 238 nm, respectively. The formulated micellar solution was mixed with anhydrous methanol before determination. Both drug loading (DL%) and encapsulation efficiency (EE%) were calculated by the subsequent equations [29]:

$$\%DL = \frac{\text{Amount of drug entrapped in } \textit{micelles}}{\text{Total weight of raw materials in micelles}} \times 100$$

$$\%EE = \frac{\text{Amount of drug actually present}}{\text{Total amount of drug added}} \times 100$$

Table I Components of the Prepared Cur-FA-MMs

Formulae code	Fusidic acid mg (w/v)	Curcumin mg (w/v)	Tween 80 g (w/v)	Lecithin g (w/v)
F1	15	80	0.25	0.04
F2	15	80	0.5	0.07
F3	15	80	0.25	0.05
F4	15	80	0.5	0.06
F5	30	80	0.25	0.04
F6	30	80	0.5	0.06
F7	30	80	0.25	0.05
F8	30	80	0.5	0.05

Selection of the Best Micellar Formula

The formula that accomplished highest % DL, % EE, and zeta potential accompanied with minimum particle size, PDI, was selected for further investigations.

Differential Scanning Calorimetry

Samples of Cur, FA, lecithin, and Cur-FA-MM optimum formula were captured and sealed in an aluminum pan with a flat-bottom crimped on lid using an empty pan as a reference (Shimadzu DSC-50, Japan). The samples were located on the sample holder and heated in the presence of nitrogen with a constant heating rate of 10 °C/min using temperature that ranged from 5 to 300°C.

Fourier Transformation Infrared Spectroscopy

For further evaluation of possible interactions between drug-excipient and excipient-excipient, potassium bromide was mixed with all tested samples at ratio 100:1 prior to examination. The IR spectra of Cur, FA, lecithin, and Cur-FA-MMs samples were detected between 400 and 4000 cm^{-1} by an IR affinity Spectrophotometer (Shimadzu, Kyoto, Japan).

Morphology Using TEM

The morphological examination was conducted for the selected micellar formula using TEM (JEOL, JEM-1230, Japan). Freshly prepared micellar dispersion was suitability diluted with 0.1M phosphate buffer and dropped onto Cu grid then marked using 2% w/v phosphotungestic acid. The stained sample was inspected, and photographs were captured with suitable magnifications [30].

In Vitro Release Study

The pattern of drugs release phosphate buffer (pH 7.4) from mixed micelles was investigated via membrane dialysis (molecular weight cutoff: 12–14 kDa, Livingstone, Sydney, Australia). Taking the sink condition in consideration, an accurate volume of pure Cur, pure FA, and Cur-FA-MMs was located into a previously hydrated dialysis bag. Dispersions of an equal content of Cur and FA were also studied. The tied dialysis bag was put into a flask containing 50 ml of phosphate buffer at 37°C and stirring 120 rpm. At planned time intervals, 1 ml of the medium was taken from the flask and replaced with 1 ml of fresh medium. The samples withdrawn were clarified through 0.22-µm Cameo Acetate membrane filter (Millipore Co., Billerica, MA), and the filtered liquid was measured spectrophotometrically at both 426 and 238 nm for detection of released Cur and FA, respectively [31].

Preparation of Cur-FA-MM-Loaded Nanogels

The selected Cur-FA-MMs were formulated as nanogel based on Abd el-Rashid *et al.* (2019) method [32]. Briefly, Carbopol 934 (1% w/w) was precisely weighed and soaked in deionized water under continuous stirring overnight until swelling. A dispersion of micellar formula was added portionwise to the swollen polymer with continuous stirring at 3000 rpm until homogeneous dispersion is obtained. By the end of the addition, an appropriate quantity of triethanolamine was added and magnetic stirring was maintained to neutralize the pH 6.8 attaining nanogel. For an efficient comparative investigation, another nanogel formula was prepared using equivalent amount of free FA and Cur suspension.

Characterization of Cur-FA-MM-Loaded Nanogels

Visual Appearance

The formulated nanogels were visually inspected for their clarity, appearance, homogeneity, and incidence of any lumps [30].

Determination of pH

An accurate amount of the prepared nanogels was dispersed in 40 ml distilled water followed by measurement of the nanogels pH via a calibrated digital Mettler Toledo MP 220 (Switzerland) [33].

Measurement of Viscosity

The viscosity of Cur-FA-MM-loaded nanogel was scrutinized using Brookfield viscometer (Brookfield DV-III, spindle 7, Ultra R/S+ Rheometer, MA, USA) at 25 ± 10 °C. The spindle of the viscometer was dripped into the nanogel and rotated at different speeds and the viscosity readings in centipoises (cps) were recorded in triplicate. For comparative purpose, the viscosity of pure drug–loaded nanogel was estimated with the same manner [34].

Ex Vivo Skin Permeation Study

Drug permeation from the prepared nanogels through skin was investigated employing Franz diffusion cells. A freshly shaved abdominal skin extracted from one rat referring to the rules of Ethical Committee of Faculty of Pharmacy, Helwan University (acceptance code 14A2022). The skin was attached between two compartments of vertical Franz diffusion cells where the stratum corneum fronted the donor compartment with 1.76 cm^2 as an actual permeation area. On the other hand, the receptor was filled with 100 mL of pH 7.4 phosphate buffer at 37 ± 0.5°C (in-simulation to blood pH) and continuously stirred at 100 rpm. One gram of Cur-FA-MM-loaded nanogel and free drug–loaded nanogel was introduced to the donor compartment. Over 24-h samples were periodically withdrawn from receptor compartment and substituted with fresh medium then evaluated for drug content spectrophotometrically at 426 and 238 nm [33, 35].

To study the deposition of Cur and FA on the rat skin after completion of permeation, a cotton cloth soaked in ethanol was used for thorough cleaning of the skin segments, followed by immersed of skin segments in ethanol for 6 h under constant stirring. The skin dispersions were then centrifuged at 5000 rpm for 20 min and clarified by 0.22-μm filter. The obtained filtrates were measured at 426 and 238 nm (UV-Visible Spectrophotometer Thermo-Scientific, USA, model Genesys 180) [36]. A curve for the cumulative amounts of drugs was plotted per unit area as a function of time to calculate the drug steady state flux (J_{ss}). The drugs permeability coefficient (kp) from Cur-FA-MM-loaded nanogel and free drug–loaded nanogel was determined as follows:

$$kp = J_{SS}/C$$

J_{ss} is the drug steady-state flux and *C* is the concentration of drug in donor compartment.

Stability of the Formed Nanogels

Cur-FA-MM-loaded nanogel stability was evaluated by storage of three samples in sealed, amber-colored screw-capped bottles for 3 months at different temperatures: 4°C, room temperature 25 °C, and 37 °C keeping humidity 75% ±5%. Obtained nanogels were visually checked at the end of storage period for appearance alteration, followed by determining drug content [32]. In order to detect statistical significance at $p < .05$, Student's *t*-test was employed using SPSS software 22.0 (SPSS Inc., Chicago, IL).

In Vivo Study

Animal studies were permitted by Faculty of Pharmacy Ethical Committee, Helwan University (acceptance code 14A2022). *In vivo* anti-acne potential of the selected Cur-FA-MM-loaded nanogel was evaluated using Rat model for acne [37–39]. The *in vivo* model shows analogous physiological events of acne genesis in rats similar to that showed in human and it is very valuable to explore the anti-acne activity of the formulated bitherapeutic micellar nanogel on the skin. The study was performed by induction of a

chronic skin inflammation using staphylococcus aureus (ATCC 29737), obtained by bacterial intradermal injection into ears of female Sprague Dawley rats weighing 150–200 g [40]. Fifty microliters of bacterial cultivates was injected intradermal to back side for rats' left ear, shaved previously, and pre-fixed using double-sided tape. In a similar way, into the right ear, 50 µL of phosphate-buffered saline was injected as a negative control. Then, a day later, constant volume of Cur-FA-MMs nanogel, free FA nanogel, and free drug combination–loaded nanogel were given topically once daily through four successive days to their animal groups. Experimental design: the rats were divided into the following 5 groups ($n = 10$): group I, negative control group; group II, positive control; group III, received fusidic acid gel; group IV taken combinatorial drug nanogel; and finally, group V, treated with Cur-FA-MM-loaded nanogel.

Determination of Anti-inflammatory Potential and Ear Thickness

Inflammatory signs as redness, pustules, lesions, or comedones on skin surface were observed. The thickness of rats' ears was measured as well using peacock dial thickness gauge [39].

Histopathological Examinations

Skin samples were taken from ear dorsum part of rats and placed in 10% formalin saline for 24h, then clipped off and desiccated in serial dilutions of alcohol, cleaned in xylol, and inserted in paraffin wax. Serial paraffin sections (6–8 µm thick) were fixed on glass slides after cutting. For histopathological inspection using electron microscope, tissue sections were dewaxed and marked by hematoxylin and eosin (H&E) dye [41]. Outcomes of histopathological were assessed by graded scores: (no abnormality) clarified by − sign, + indicates (mild), ++ referred (moderate) fluctuations observed in the investigated smears [42].

Statistical Analysis

Obtained results of different investigations examined by paired sample *t*-test for significant difference at $p < 0.05$ utilizing SPSS 16.0 program (Chicago, IL, USA).

Results and Discussion

Validation of UV-Spectrophotometric Method for Determination of Drugs

Screening for Cur and FA showed that each of them had a unique characteristic peak that does not overlap with the other (Fig. 1). Cur and FA were measured at λ max of 426 nm and 238 nm, respectively. Standardization curves of both drugs in either methanol or phosphate buffer (pH=7.4) followed Beer's
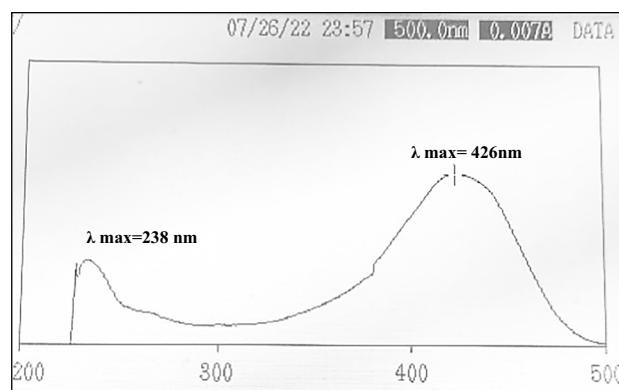

Fig. 1 UV-spectrum illustrate the distinctive peaks of FA at λ max=238nm and Cur at λ max= 426nm

law in range of 5–40 mg/ml for FA and 0.5–5 µg/ml for Cur with a regression coefficient (R^2) of approximately 0.999. The percentage recovery was ranged between 98 and 103% for both drugs in their either free or binary form at different concentrations. The low values of standard deviation and % relative standard deviation (<1%) were confirmed high precision and accuracy of the determination method.

Micelle Size, PDI, and Zeta Potential

Micelle size, PDI, and ZP results for the formulated Cur-FA-MMs were presented at Table II. The obtained sizes strongly allow efficient drug delivery, drug deposition, and permeability to biological cell owing to their nanometric size range [43]. The mean size for Cur-FA-MMs ranged from 58 ± 3.63nm and 95±1.63nm. The Cur-FA-MM formulas (F5, F6, F7, and F8) displayed an increase in average particle size compared to F1, F2, F3, and F4 owing to the high concentration of FA incorporated and possible hydrophobic–hydrophobic interaction of FA and lecithin at constant Cur concentration [44]. The results obviously displayed that the micelles' average size decreased as the concentration of surfactant (Tween 80) increased which mainly correlated to Tween 80 ability to narrow the micelle size with more uniform size and shape by high stabilization to the system formed efficiently [45]. Also the presence of lecithin was good for Cur as well as FA, and accomplished good solubilization and appropriate self-emulsification which attained small micelle size [46]. Both Tween 80 and lecithin complete each other to form stable micelle; Tween 80 has high tendency to form stable micelle by reducing electrostatic repulsion between present ionic heads of lecithin, hence declining critical micelle concentration (CMC) [47]. All the developed micelles also revealed narrow size distributions with uniformity, homogeneity, and physical stability due to their PDI values which ranged from 0.2 to 0.54

Estimating risk of micelles aggregation could be easily detected by the assessment of the zeta potential [48]. The

Table II Micellar Size, PDI, Zeta Potential (ZP), DL%, and EE% of Cur-FA-MMs

Formulations	Micellar size	PDI	ZP	% DL		% EE	
				Cur	FA	Cur	FA
F1	78±2.9	0.29±2.4	−19±1.66	18±1.8	5.7±1.4	63.5±1.2	66± 3.2
F2	58± 3.63	0.22±1.5	−34.5±1.8	21.5±2	9.5±2.1	85± 0.79	88±3.7
F3	80±3.33	0.33±2	−27.8±2.4	17±1.77	6 ±1.2	65±0.9	59±1.7
F4	68±1.9	0.46±1.9	−22.5±1.64	11.8±2	5 ±1.5	80±0.85	71±2
F5	90±0.67	0.54±0.98	−30.2±1.98	16±2.34	8 ±1.6	70±1.8	65.3±3.1
F6	78±2.6	0.37±1.55	−26.4±0.87	10.5±2	6.4±2.1	72±0.58	73±2.8
F7	95±1.63	0.45±2	−20.7±2	14±1.88	7.8±0.78	59±0.65	52.5±3.1
F8	79±1.87	0.51±2.2	−23.1±2.23	9.5±0.9	7±0.99	67±1.9	75.5±1.66

negative surface charge for Cur-FA-MMs was extended between −18± 2.1 and −35± 3.72 mV which may be ascribed to phosphatidylcholine amphiphilic surfactant. The higher negativity for surface charge values for developed micelles suggested high resistance against aggregation and good stability. Beside the electrostatic repulsion, interactions among other hydrophilic chains of prepared mixed micellar system might inhibit micelle accumulation affording stability for the system [47].

Efficiency of Entrapment (EE %) and Drug Loading (DL %) for Fabricated Cur-FA-MMs

The EE % as well as DL% of Cur and FA among obtained micelles is displayed at Table II. The fabricated Cur-FA-MMs profit high DL% (5±1.5 to 21.5±2) for both Cur and FA. The high loading capacity related to the drugs' lipid solubility and their hydrophobic–hydrophobic interaction with micelle core forming interpenetrated network chain capture drugs deeply. The % EE for Cur was extended between 59± 0.65 and 85 ± 0.79 and the % EE for FA was within the range of 52.5±3.1 to 88 ± 3.72. Generally, the high % EE of both Cur and FA could be due to their high lipophilicity (log P 2.5 and log P 5.2, respectively) which fruitfully encapsulated into the mixed micelles pulp cavity [49]. The results clarified that the % EE for both Cur and FA increased by increasing Tween 80 concentrations which generally shrinkage surface tension of combined polymer and consequently increase the encapsulating efficiency. Besides, the high solubilization capacity of Cur and FA with the longer hydrophobic chain of lecithin attained higher compatibility with inner core of the formulated micellar system and hence high DL% and EE% [50]. Moreover, the high chemotactic between Cur and FA and lecithin allowed them to embedded firmly into the inner hydrophobic core compartment [24, 51]. Additionally, the tendency of Tween 80 in reducing repulsion between ionic heads and lower CMC consequently increase intermolecular polymerization.

Best Formula Selection

The principles for election were depending on earning (high %DL and EE% with smallest size, PDI, and ZP). According to previous results, F2 could be elected as prime Cur-FA-MMs as it revealed small values in size (58 nm), and PDI (0.22) as well as ZP (−34.5mV) which consequently harmonized with maximum %EE (85% and 88% for Cur and FA, respectively, Table II). This could be attributed to the affinity of the lecithin/Tween 80 mixed micelle as a nanocarrier to embed natural and lipophilic drugs into inner hydrophobic core which afford high space capacity for drug encapsulation, and maximize therapeutic efficacy with optimum stability. Therefore, F2 was subjected to subsequent investigations.

Compatibility Studies

DSC

Figure 2 shows pure Cur, FA, lecithin, and selected Cur-FA-MMs (F2) thermograms. Differential scanning calorimetry (DSC) thermograms of pure Cur and pure FA showed a sharp endothermic peak at 186°C and 188°C, respectively referring to their characteristic melting points [52, 53]. The sharp endothermic peaks of pure drugs proposed their pure crystalline states. The thermogram of the optimum Cur-FA-MMs displayed complete disappearance of both Cur and FA characteristic peaks revealing that drug molecules were encapsulated inside the micelle hydrophobic core in amorphous or molecular form which subsequently indicates absence of unentrapped drug on the surface of micelle.

FTIR

Pure Cur, FA, and lecithin as well as optimum Cur-FA-MMs (F2) Fourier transformation infrared spectroscopy (FTIR) spectra are demonstrated in Fig. 3. FTIR band for free Cur was characterized by an intense peak at 3509 cm^{-1} related to stretching vibration of phenol-OH. The C=O and C=C stretching
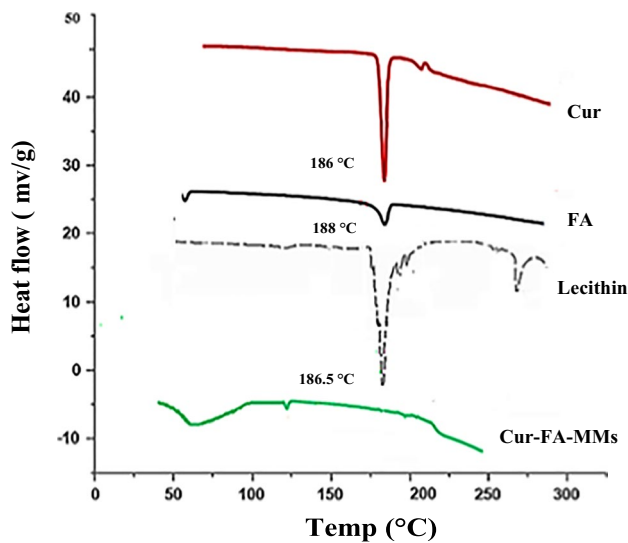
Fig. 2 DSC thermograms of free Cur, FA, lecithin, and selected Cur-FA-MMs

Fig. 4 TEM image of the optimum Cur-FA-MMs

vibrations were also noted at 1628 cm^{-1} [53]. For FA spectrum, large vibration with great intensity observed at 3446 cm^{-1} allied to O–H bond stretching. Besides, both stretching of C=O (symmetrical and asymmetrical) with intense vibrations at 1686 and 1742 cm^{-1} were also detected [54]. In lecithin spectrum, symmetric CH$_2$ alkane bonds at 2854 cm^{-1} and asymmetric for CH$_2$ at 2928 cm^{-1} were demonstrated. Other intense band was located at 3400cm^{-1} associated with the stretching vibrations of –OH in carboxylate. The selected Cur-FA-MM spectrum exhibited the same site for free Cur and FA characteristic peaks without any changes settling no interaction possibly occur among drugs and other excipients.

TEM

A demonstrative TEM photomicrograph of optimum Cur-FA-MMs (F2) is clarified in Fig. 4. The micelles were like

unilamellar disc with scattered rod-like particles formed due to lecithin-Tween 80 mixed micelle formation. The TEM examination also revealed almost uniform tiny spherical size or spheroid look with high homogeneity. Attained result was consistent with zeta sizer records.

In Vitro Release Study

To simulate *in vivo* process, the *in vitro* release study was accomplished as a mirror. As shown in Fig. 5, both Cur and FA displayed slow release from Cur-FA-MMs (F2) over a period up to 48h; only 39% and 41% of Cur and FA, respectively, were released from MMs within the first 6 h. On contrast, more than 80% of the Cur and FA were released from their suspensions during the same time. The Cur-FA-MMs release displayed a biphasic pattern with initial burst % release of 30 ± 2.4 and 34 ± 1.9 for Cur and FA, respectively, followed by sustained release up to 48h. Primarily, rupture effect could be attributed to accelerate release of little amount of drugs (Cur and FA) fixed at the outer hydrophilic shell of

Fig. 3 FTIR of pure Cur, FA, lecithin, and optimized Cur-FA-MMs
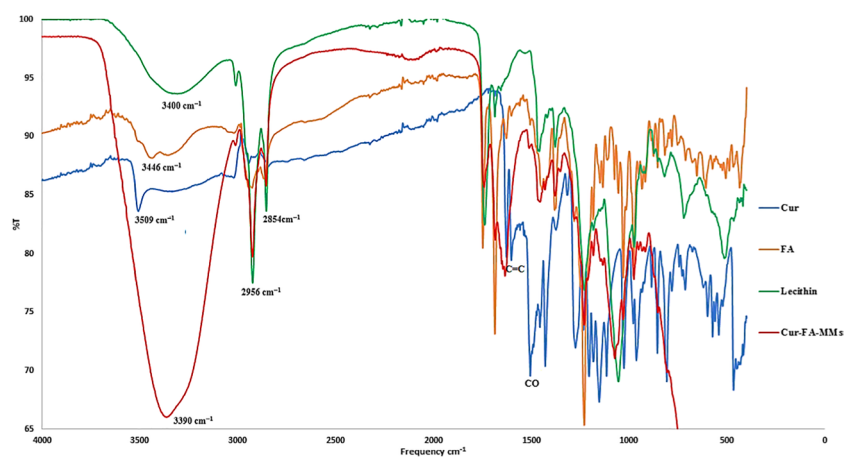
Fig. 5 *In vitro* release profiles for Cur, and FA, from their free dispersions compared to Cur-FA-MM formulations
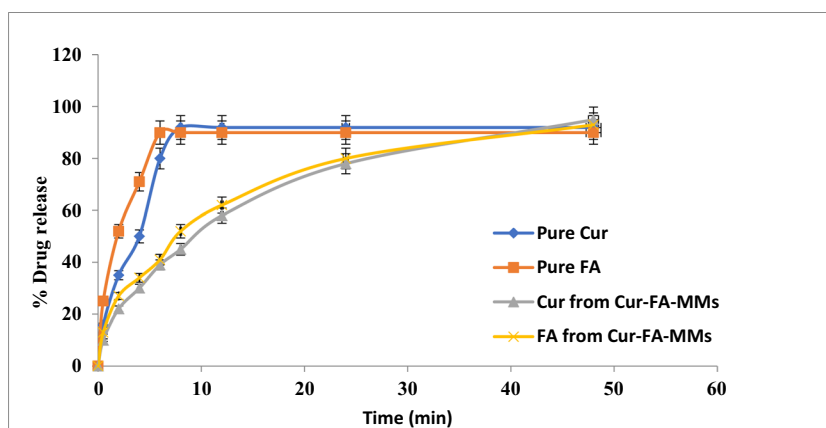
the micelle, while the sustained release could be associated with most Cur and FA embedded into the inner hydrophobic core compartment via hydrophobic interaction and/or hydrogen bonds make them persisted inside micelle firmly presenting delay release [51]. Additionally, the amorphous state as confirmed by the DSC of Cur and FA inside the mixed micelle encourages sustained release [55]. The released mechanism of both Cur and FA from micelle might be allied to the drug diffusion as well as polymer swelling and degradation [27]. Moreover, the release of Cur with FA at the same time could make boosted effects on FA. The slow sustained release modality of bitherapeutic from mixed micelle is beneficial in enhancing drug residence, and lessening the times of administration eliminating annoyance from direct contact between drug and skin improving patient compliance [56].

Characterization of Cur-FA-MM-Loaded Nanogel

Visual Appearance

Figure 6a and b illustrate the visual inspection of free drug combination and micellar nanogels. The micellar nanogel exhibited light yellow color with elegant transparent appearance with clear lack of lumps and aggregations. High homogeneity, excellent consistency, and absence of phase separation were also detected (Fig. 6a). On the contrary, the free drug nanogel was turbid, and coalesced, with non-homogenous dull appearance and low consistency (Fig. 6b).

pH and Viscosity

The obtained pH for nanogels was extended from 5.7 to 6.2 that agreed with skin pH excluding the risk of skin irritation [57]. Besides, values obtained were adequate to obtain clear and transparent gels with optimum viscosity [58]. Hence, the prepared nanogel was suitable for topical applications.

The viscosity has a direct relationship with spreadability and rheology of the gel affording good expectations for gels residence time. The Cur-FA-MM nanogel formulation viscosity was $13,355 \pm 200$ (cP) that fulfills with recognizable viscosity range of gel 13,000–16,000 (cP) [59], while the free drug nanogel showed high viscosity $19,850 \pm 300$ (cP) which adversely impacts the rate of drug released reducing its availability for skin permeation. The results clarified the positive effect of mixed micelles on the rheological properties of the gel formulation assisting spreadability and retention on the skin [60].

Fig. 6 a, b Visual appearance of Cur-FA-MM nanogel and free drug nanogel

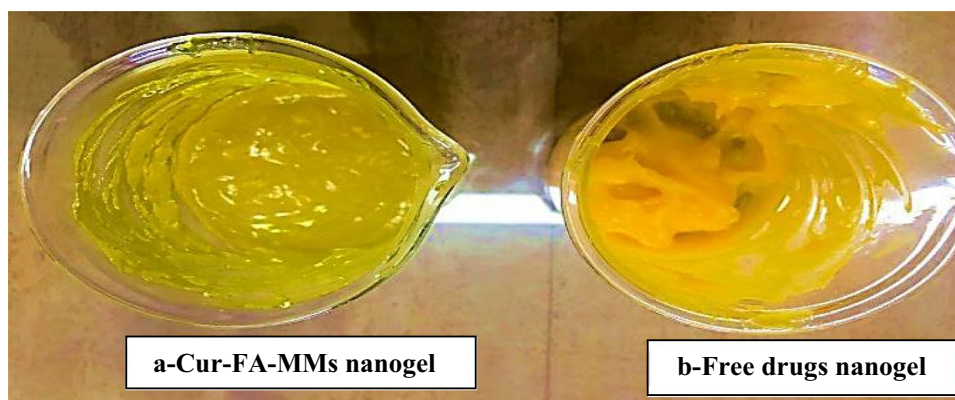a-Cur-FA-MMs nanogel   b-Free drugs nanogel

Table III Drug Content (%) of Formulated Cur-FA-MM Nanogel through Storage Period (3 months) at Different Temperatures 4°C, 25°C, and 37°C in Relative Humidity 75±5%

Parameters	Cur-FA-MM nanogel					
	Storage period (temperature/months)					
	4°C		25°C		37°C	
	0	3	0	3	0	3
% drug content	97.8	97.3	96.5	96.1	93.9	79.7

Short-Term Stability

After storage period (3 months) at 4°C, 25°C as well as 37°C, Cur-FA-MM nanogel kept its clear, elegant, and transparent appearance with no color change and sedimentation observed. The drug contents at 4°C and 25°C were statistically insignificant ($p>.05$, paired t-test) with results acquired before storage (Table III) that proved micellar nanogel formulation stability. However, a remarkable decrease in content was noticed for one kept at 37 °C which agreed with results obtained in previous study [32].

Ex Vivo Permeation

Ex vivo model (Rat model, 150–200 g) that used animal skin has been applied among various research studies as successful mimic for human skin. Accordingly, a rat skin

Fig. 7 Concentrations of **a** FA and **b** Cur permeated skin from both prepared formula and plain nanogel

was selected for studying the effect of drug delivery system (mixed micelles in nanogel) on permeation and deposition of FA and Cur combination [52, 61]. Both FA and Cur cumulative permeated amount with abdominal rat skin unit area, as well as Cur-FA-MM nanogel compared with free drug nanogel is exhibited in Fig. 7a and b while the parameters of permeation are shown in Table IV.

Obviously, biphasic release pattern was detected for both drugs which coincide with *in vitro* release study results (Fig. 7). After the first hour, large amounts of Cur and FA from both formulation and plain nanogel were measured (1158.49, 707.76, 574.81, and 246.33 µg/ml, respectively). As clearly shown, the permeation of both FA and Cur from plain nanogel through rat skin was significantly low ($p<0.05$) in comparison to Cur-FA-MMs nanogel. Encapsulation of drugs in mixed micelles has shown nearly 2-fold permeation enhancement related to plain nanogel. The effect of delivery system was also quite apparent on the values of permeation coefficient demonstrated by Cur-FA-MM nanogel (0.043, 0.051 cm/h for Cur and FA, respectively) related to plain nanogel (0.009, 0.0104 cm/h for FA and Cur, respectively) as shown in Table IV. The results could be owing to mixed micellar formulation components (lecithin and Tween 80) which are known of their permeation enhancement activity. Furthermore, the high permeation through skin for 2 drugs could also be explained by the entrapment of drugs in nanosized structure with high flexibility owing to the presence of surfactant which enables drug permeation through successive skin layers [35, 62].

From the data presented in Table IV, it could also be clearly deduced the higher amount of drug combination retained in skin for Cur-FA-MM nanogel compared to plain nanogel; this agreed with the nature of the mixed micelle
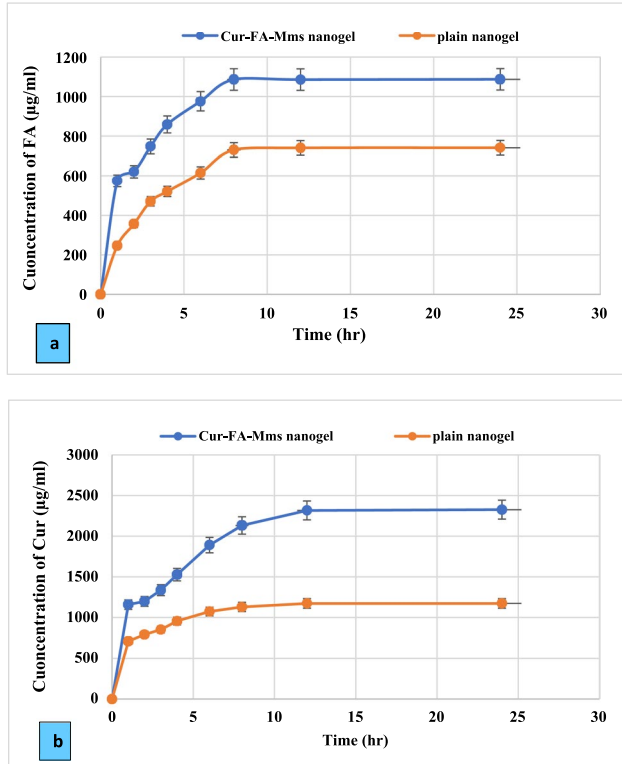
Table IV *Ex vivo* Parameters for Micllar and Free Drugs Nanogels

Item	Cur-FA-MM nanogel		Free drug nanogel	
	FA	Cur	FA	Cur
Amount deposited in skin (ug/cm²)	405.47	562.07	197.79	308.62
Jss (ug/cm²·h)	74.5	85.71	38.71	49.5
Permeability coefficient (cm/h)	0.043	0.051	0.009	0.0104

and its ability to pass through cell membranes. The amounts of drugs deposited was 405.47 and 562.07 ug/cm^2 for FA and Cur from Cur-FA-MM nanogel, respectively, while FA and Cur deposited from plain nanogel were 197.79 and 308.62 ug/cm^2, respectively.

In Vivo Study

Determination of Anti-inflammatory Potential and Ear Thickness

In comparison to the negative control (group I), the inflammation could be detected as a marked increase in both thickness and redness of the ear of all groups treated with *Staphylococcus aureus*. Meanwhile, groups IV and V faced a significant reduction in inflammation signs as shown in Fig. 8. It was also found that reduction of inflammation (ear thickness) was 70% for group V (treated with Cur-FA-MM nanogel) compared to 47.2% for plain nanogel (group IV) and 30% for group III (treated with fusidic acid gel). Additionally, group III

showed least anti-inflammatory potential which could be justified by the absence of Cur *additive* effect. Consistently, these results were reinforced via preclinical studies performed by *Liu and Huang, 2012*, in rat model of acne vulgaris which showed that Cur may have strong antibacterial and antioxidant properties leading to significant reduction of inflammatory cytokine as well as comedone production [63].

Furthermore, the results emphasized the effect of dual delivery for both FA (antibacterial) and Cur (antioxidant with reported antibacterial activity) at the same site of administration on reducing the risk of emerging antibiotic resistance.

The mixed micellar nanogel could also has a strong activity in improving anti-inflammatory effects of Cur/FA combination by elevating their stratum corneum penetration; adhesion firmly on skin surface by its occlusive effect permits the active controlled release increasing effective concentration of encapsulated drugs [64]. In Fig. 8, the visual inspection of rat ears showed the excessive appearance of redness and papules on day 2
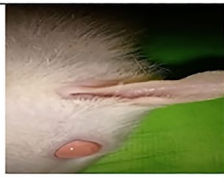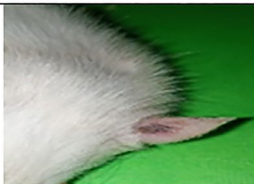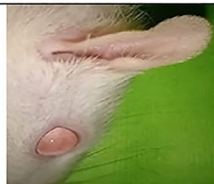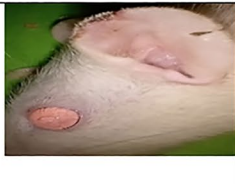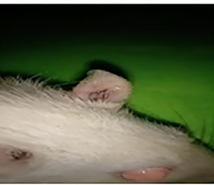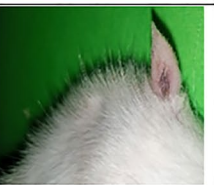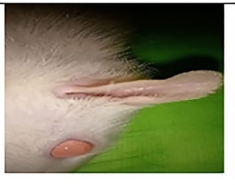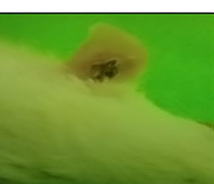

	Group I (Negative control)	Group II (Positive control)	Group III (Fusidic acid gel)	Group IV (Plain nanogel)	Group V (Cur-FA-MMs nanogel)
Day 1					
Day 2					
Day 4					

Fig. 8 Macroscopic morphological changes in rat ear model for detection of ant-inflammatory potential

Table V Histopathological Findings of Rat Ear Skin

Groups	Group I			Group II			Group III			Group IV			Group V		
Number of examined fields	10														
Grade	–	+	++	–	+	++	–	+	++	–	+	++	–	+	++
Abnormal changes															
Inflammatory cell infiltration	8	2	0	0	5	5	3	7	0	4	6	0	6	4	0
Thick epidermis (hypertrophy)	9	1	0	1	4	5	3	5	2	6	4	0	7	3	0
Dermal congestion	10	0	0	0	3	7	2	7	1	1	5	4	5	5	0

*Grade of histopathological findings: – (no abnormality), + (slight), ++ (mild)

for group II (positive control). On the other hand, the group treated with Cur-FA-MMs nanogel showed the least inflammation signs.

Histopathological Examination

The histopathological findings showed least abnormalities detected for the group treated with Cur-FA-MM nanogel compared to other groups as shown in Table V and Fig. 9. The examination of group II (positive control) showed high invasion of inflammatory cells in the dermis layer. The dermis layer showed significant congestion and disarray. Epidermal cells exhibited a moderate hyperplasia, and some regions displayed typical epidermal thickness with vacuolated epithelial cells with shrinking darkly pigmented nuclei. A few places showed many hair follicles with atrophy sebaceous gland. However, the group treated with fusidic acid gel showed invasion of inflammatory cells occurred in the dermal layer at a moderate level. Dermis showed moderate congestion, certain sebaceous glands being destroyed.

The histopathological features of skin treated with combination drugs nanogel (group IV) showed a slight enlargement of the epidermal cells thickness, and there appeared to be more epidermal cells overall (hyperplasia). Most of the epidermal layers displayed normal thickness and were covered by thick keratin layers. In the group treated with Cur-FA-MM nanogel, the dermis, the layer of tissue under the skin, showed a minimal amount of congestion and inflammatory cell infiltration. Many hair follicles were ordinarily connected to sebaceous glands. Nearly typical thickness of the epidermal layer was noted.

In conclusion, after being treated with Cur-FA-MM nanogel, the skin's degree of inflammatory cell infiltration, epidermal hypertrophy, and congestion were improved. The results confirmed the benefits of combinatorial delivery of Cur and FA from a highly permeable delivery system for successful treatment of acne vulgaris.

Conclusion

Considering the prospective of combination therapy as an emerging strategy for overwhelming the settle side effects and bacterial resistance, this study involved preparation and characterization of mixed micelles (MMs) incorporated into nanogel as nanocarrier for delivery of FA and Cur combination to expand antibacterial efficiency of FA. Cur-FA-MMs were successfully formulated with uniform spherical morphology and high %EE for both Cur and FA, displaying a biphasic release pattern. The Cur-FA-MM
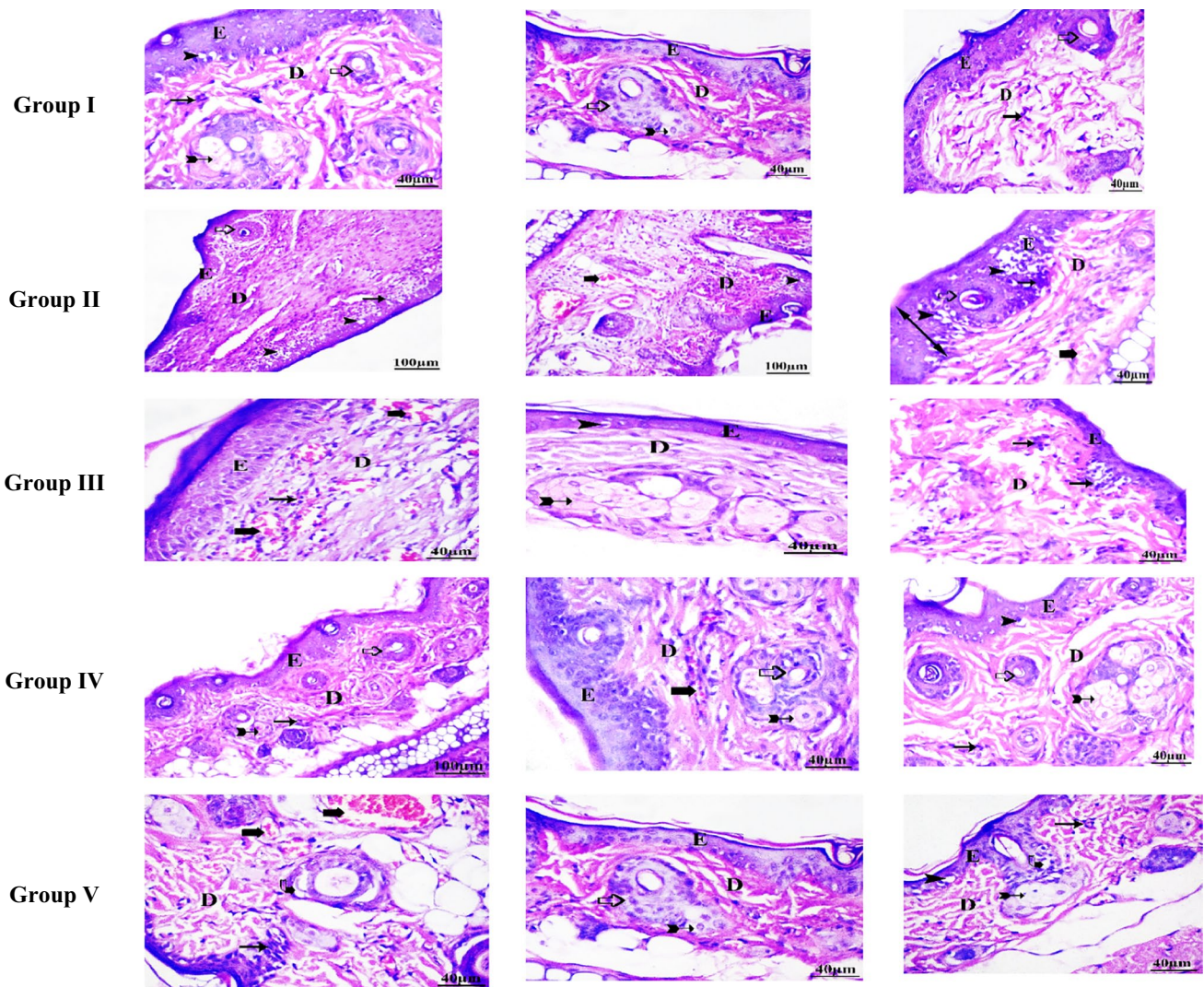
Fig. 9 Histopathological examination of rat ear skin by the end of experimental study. *Group I* (negative control), epidermis (E), normal dermis (D), hair follicle, and epithelial cells are healthy. *Group II* (positive control) epidermis (E), disordered dermis (D), hair follicle (hollow arrow), Congestion (bold arrow), vacuolated epithelial cell (head arrow), cellular infiltration in the dermis (arrow), epithelial hyperplasia (double head arrow), sebaceous gland (bifid arrow), degenerated epithelial cells formed hair follicle (curved arrow). *Group III* (fusidic acid gel) epidermis (E) mild inflammatory cells, disordered dermis (D), congestion (moder-ate), vacuolated epithelial cell (head arrow). *Group IV* (plain drug combination nanogel) epidermis (E), dermis (D), congestion (bold arrow), vacuolated epithelial cell (head arrow), mononuclear cellular infiltration in dermis (arrow), hair follicle (hollow arrow), sebaceous gland (bifid arrow), vacuolated epithelial cells formed hair follicle (curved arrow). *Group V* (Cur-FA-MMS nanogel) epidermis (E), dermis (D), intact hair follicle (hollow arrow), congestion (bold arrow very low), cellular infiltration in the dermis (minimal), integral sebaceous gland (bifid arrow), vacuolated epithelial cell (absent)

nanogel showed 2-fold permeation enhancements with low inflammation signs free from redness and papules which scrutinized in rats ears. The study suggests that the co-delivery of FA (antibiotic) and Cur (antioxidant with reported antibiotic activity) in mixed micelle nanocarrier could emphasize the *boosted* effect for both drugs at the same site of administration decreasing the risk of emerging antibiotic resistance.

Data availability All data supporting the findings of this study and materials are available.

Declarations

Institutional Review Board Statement The study protocol was performed after the approval of the Animal Ethics Committee of Faculty of Pharmacy, Helwan University (Acceptance code 14A2022).

Authors' Declaration All authors have carefully read and adhered to all the guidelines and instructions to authors provided in the ARRIVE guidelines.

Approval for Publication All authors read and approved the published version of the manuscript.

Competing Interests The authors declare no competing interests.

References

1. Yang JH, Yoon JY, Kwon HH, Min S, Moon J, Suh DH. Seeking new acne treatment from natural products, devices and synthetic drug discovery. Dermato Endocrinol. 2017;9:1356520.

2. Joshi D, Bahuguna S, Sharma P, Singh B, Semwal N. Novel approaches in herbal medicament for acne vulgaris. JOJ Dermatol & Cosmet. 2022;4.

3. Nakatsuji T, Liu Y, Huang C, Zoubouis CC, Gallo RL, Huang C. Antibodies elicited by inactivated propionibacterium acnes-based vaccines exert protective immunity and attenuate the IL-8 production in human sebocytes: relevance to therapy for acne vulgaris. J Invest Dermatol. 2008;128:2451–7.

4. Chakraborty N, Narayanan V, Gautam HK. Nano-therapeutics to treat acne vulgaris. Indian J Microbiol. 2022;62:167–74.

5. Qadir A, Ullah SNMN, Gupta DK, Khan N. Phytoconstituents-loaded nanomedicines for the management of acne. J Cosmet Dermatol. 2022;21:3240–55.

6. Paiva-Santos AC, Mascarenhas-Melo F, Coimbra SC, Pawar KD, et al. Nanotechnology-based formulations toward the improved topical delivery of anti-acne active ingredients. Expert Opin Drug Deliv. 2021;18:1435–54.

7. Tobiaz A, Nowicka D, Szepietowski JC. Acne vulgaris-novel treatment options and factors affecting therapy adherence: a narrative review. J Clin Med. 2022;11:7535.

8. Sabouri M, Samadi A, Nasrollahi SA, et al. Tretinoin loaded nanoemulsion for acne vulgaris: fabrication, physicochemical and clinical efficacy assessments. Skin Pharmacol Physiol. 2018;31:316–23.

9. Mohsin N, Hernandez LE, Martin MR, Does AV, Nouri K. Acne treatment review and future perspectives. Dermatol Ther. 2022;35:e15719.

10. Moura IB, Grada A, Spittal W, Clark E, et al. Profiling the effects of systemic antibiotics for acne, including the narrow-spectrum antibiotic sarecycline, on the human gut microbiota. Front Microbiol. 2022;13:901911.

11. Wadhwa S, Singh B, Sharma G, Raza K, Katare O. Liposomal fusidic acid as a potential delivery system: a new paradigm in the treatment of chronic plaque psoriasis. Drug Deliv. 2016;23:1204–13.

12. Al Mostafa MM, El Sewedy HS, Shehata TM, Soliman WE. Novel formulation of fusidic acid incorporated into a myrrh-oil-based nanoemulgel for the enhancement of skin bacterial infection treatment. Gels. 2022;8:245.

13. Tu B, Cao N, Zhang B, Zheng W, Li J, Tang X, Su K. Synthesis and biological evaluation of novel fusidic acid derivatives as two-in-one agent with potent antibacterial and anti-inflammatory activity. Antibiotics (Basel). 2022;11:1026.

14 El-Leithy ES, Ab del-Rashid RS. Lipid nanocarriers for tamoxifen citrate/coenzyme Q10 dual delivery. J Drug Deliv Sci Technol. 2017;41:239-e250.

15. Hajheydari Z, Saeedi M, Morteza-Semnani K, Soltani A. Effect of Aloe vera topical gel combined with tretinoin in treatment of mild and moderate acne vulgaris: a randomized, double-blind, prospective trial. J Dermatolog Treat. 2014;2:123–32.

16. Menon S, Vartak R, Patel K, Billack B. Evaluation of the antifungal activity of an ebselen-loaded nanoemulsion in a mouse model of vulvovaginal candidiasis. Nanomedicine: Nanotechnology, Biology and Medicine. 2021;(37):102428.

17. Proença AC, Luís A, Duart AP. The role of herbal medicine in the treatment of acne vulgaris: a systematic review of clinical trials. Evid Based Complement Alternat Med. 2022;2011945.

18. Fluoria S, Mehta J, Chandel A, Sekar M, Rani NNIM, et al. A comprehensive review on the therapeutic potential of *Curcuma longa* Linn in relation to its major active constituent curcumin. Front Pharmacol. 2022;13:820806.

19. Akbar MU, Rehman K, Zia KM, Qadir MI, et al. Critical review on curcumin as a therapeutic agent: from traditional herbal medicine to an ideal therapeutic agent. Crit Rev Eukaryot Gene Expr. 2018;28:17–24.

20. Jyotirmayee B, Mahalik G. A review on selected pharmacological activities of Curcuma longa L. Int J Food Prop. 2022;25:1377–98.

21. Vollono L, Falconi M, Gaziano R, Iacovelli F, Dika E, et al. Potential of curcumin in skin disorders. Nutrients. 2019;11:2169.

22. Suresh MV, Francis S, Aktay S, et al. Therapeutic potential of curcumin in ARDS and COVID-19. Clin Exp Pharmacol Physiol. 2023;50:267–76.

23. Tănase MA, Raducan A, Oancea P, Ditu LM, Stan M, Petcu C, et al. Mixed pluronic-cremophor polymeric micelles as nanocarriers for poorly soluble antibiotics-the influence on the antibacterial activity. Pharmaceutics. 2021;13:435.

24. Bothiraja C, Kapare HS, Pawar AP, Shaikh KS. Development of plumbagin-loaded phospholipid-Tween® 80 mixed micelles: formulation, optimization, effect on breast cancer cells and human blood/serum compatibility testing. Ther Deliv. 2013;4:1247–59.

25. Seo SH, Kim E, Joo Y, Lee JOH, et al. A mixed micellar formulation for the transdermal delivery of an Indirubin Analog. Pharmaceutics. 2020;12:175.

26. Duan J, Wang X, Yang H, Du H, Xi G. Zhai, Curcumin-loaded mixed micelles: preparation, optimization, physicochemical properties and cytotoxicity in vitro. Drug Deliv. 2015;22:50–7.

27. Nasr M, Hashem F. Abd el moniem R, Tantawy N, Teiama M, In vitro cytotoxicity and cellular uptake of tamoxifen citrate-loaded polymeric micelles. AAPS Pharm Sci Tech. 2020;21:306.

28. Abdellatif AAH, Tawfeek HM. Transfersomal nanoparticles for enhanced transdermal delivery of clindamycin. AAPS Pharm Sci Tech. 2016;17:1477–94.

29. Abo El-Enin HA, Ahmed MF, Naguib IA, El-Far SW, et al. Utilization of polymeric micelles as a lucrative platform for efficient brain deposition of olanzapine as an antischizophrenic drug via intranasal delivery. Pharmaceuticals. 2022;15:249.

30. Sakran W, Abdel-Rashid RS, Saleh F, Abdel-Monem R. Ethosomal gel for rectal transmucosal delivery of domperidone: design of experiment, in vitro, and in vivo evaluation. Drug Deliv. 2022;29:1477–91.

31. Upadhayay P, Kumar M, Pathak K. Norfloxacin loaded pH triggered nanoparticulate in-situ gel for extraocular bacterial infections: optimization, ocular irritancy and corneal toxicity. Iran J Pharm Res. 2016;1:3–22.

32. Abdel-Rashid RS, Helal DA, Omar MM, El Sisi AM. Nanogel loaded with surfactant based nanovesicles for enhanced ocular delivery of acetazolamide. Int J Nanomedicine. 2019;14:2973–83.

33. Ismail TA, Shehata TM, Mohamed DI, et al. Quality by design for development, optimization and characterization of brucine ethosomal gel for skin cancer delivery. Molecules. 2021;26:3454.

34. Tiwari A, Bag P, Sarkar M, et al. Formulation, validation and evaluation studies on metaxalone and diclofenac potassium topical gel. Environ Anal Health Toxicol. 2021;36:e2021001.

35. Nawaz A, Farid A, Safdar M, Latif MS, Ghazanfar S, et al. Formulation development and ex-vivo permeability of curcumin hydrogels under the influence of natural chemical enhancers. Gels. 2022;8:384.

36. Shahid M, Hussain A, Khan AA, Alanazi AM, Alaofi AL, Alam M, Ramzan M. Antifungal cationic nanoemulsion ferrying miconazole nitrate with synergism to control fungal infections in vitro, ex vivo, and in vivo evaluations. ACS Omega. 2022;7:13343–53.

37. Białecka A, Mak M, Biedroń R, Bobek M, et al. Different pro-inflammatory and immunogenic potentials of Propionibacterium acnes and Staphylococcus epidermidis: implications for chronic inflammatory acne. Arch Immunol Ther Exp. 2005;53:79–85.

38. Rottboell L, De Foenss S, Thomsen K, Christiansen H, Andersen SM, Dam TM. Exploring valrubicin's effect on propionibacterium acnes-induced skin inflammation in vitro and in vivo. Dermatol Reports. 2015;7:6246.

39. Kanwar IL, Haider T, Kumari A, Dubey S, et al. Models for acne: a comprehensive study. Drug Discov Ther. 2018;12:29–340.

40. Nazeam JA, Ragab GM, El-Gazar AA, El-Mancy SS, Jamil L, Fayez SM. Topical nano clove/thyme gel against genetically identified clinical skin isolates: in vivo targeting behavioral alteration and IGF-1/pFOXO-1/PPAR γ cues. Molecules. 2021;26:5608.

41. Bassiony H, El-Ghor AA, Salaheldin TA, Sabet S, Mohamed MM. Tissue distribution, histopathological and genotoxic effects of magnetite nanoparticles on Ehrlich solid carcinoma. Biol Trace Elem Res. 2022;12:5145–58.

42. Watanabe T, Hamada K, Tategaki A, Kishida H, Tanaka H, et al. Oral administration of lactic acid bacteria isolated from traditional South Asian fermented milk "dahi" inhibits the development of atopic dermatitis in NC/Nga mice. J Nutr Sci Vitaminol (Tokyo). 2009;55:271–8.

43 Abdel-Rashid RS, Helal DA, Alaa-Eldin AA, Abd el moneum R. Polymeric versus lipid nanocapsules for miconazole nitrate enhanced topical delivery: in vitro and ex vivo evaluation. Drug Deliv. 2022;29:294–304.

44. Song H, Geng H, Ruan J, Wang K, Bao C, Wang J, Peng X. Development of Polysorbate 80/phospholipid mixed micellar formation for docetaxel and assessment of its in vivo distribution in animal models. Nanoscale Res Lett. 2011;6:354.

45. Joseph D, Lee H, Huh YS, Han Y. Cylindrical core-shell Tween 80 micelle templated green synthesis of gold-silver hollow cubic nanostructures as efficient nanocatalysts. Materials & Design. 2018;160:169–78.

46. Kamel R, Basha M. Preparation and in vitro evaluation of rutin nanostructured liquisolid delivery system. Bull Fac Pharm Cairo Univ. 2013;51:261–72.

47. Chen L, Chen Y, Su C, Wong W, Sheu M, Ho H. Development and characterization of lecithin-based self-assembling mixed polymeric micellar (saMPMs) drug delivery systems for curcumin. Sci Rep. 2016;6:37122.

48. Le Guyader G, Do B, Rietveld IB, Coric P, Bouaziz S, et al. Mixed polymeric micelles for rapamycin skin delivery. Pharmaceutics. 2022;14:569.

49. Zong S, Liu Y, Park HJ, Ye M, Li J. Curcumin solid dispersion based on three model acrylic polymers: formulation and release properties. Braz J Pharm Sci. 2022;58:e1894.

50. Vinarov Z, Gancheva G, Burdzhiev N, Tcholakova S. Solubilization of itraconazole by surfactants and phospholipid-surfactant mixtures: interplay of amphiphile structure, pH and electrostatic interactions. J Drug Deliv Sci Technol. 2020;57:101688.

51. Zhou Y, Zhou CY, Zou Y, et al. Multi pH-sensitive polymer-drug conjugate mixed micelles for efficient co-delivery of doxorubicin and curcumin to synergistically suppress tumor metastasis. Biomater Sci. 2020;18:5029–46.

52. Ahmed IS, El Nahas OS, Assar NH, Gad AM, El Hosary R. Nanocrystals of fusidic acid for dual enhancement of dermal delivery and antibacterial activity: in vitro, ex vivo and in vivo evaluation. Pharmaceutics. 2020;12:199.

53 Xie H, Ma L, Li Y, Fu J, Li Z, Yu Z, Gao M. Preparation and characterizations of curcumin protection and delivery system using linear dextrin. Compounds. 2022;2:353–66.

54. Marian E, Tita B, Duteanu N, Vicas L, Ciocan S, Jurca T, Antal L. Antimicrobial activity of fusidic acid inclusion complexes. Int J Infect Dis. 2020;101:65–73.

55. Gupta T, Singh J, Kaur S, Sandhu S, Singh G, Kaur IP. Enhancing bioavailability and stability of curcumin using solid lipid nanoparticles (CLEN): a covenant for its effectiveness. Front Bioeng Biotechnol. 2020;15:879.

56. Bose A, Burman DR, Sikdar B, Patra P. Nanomicelles: types, properties and applications in drug delivery. IET Nanobiotechnol. 2021;15:19–27.

57. Al Moshari Y. Novel hydrogels for topical applications: an updated comprehensive review based on source. Gels. 2022;2:174.

58. Dantas MGB, Reis SAGB, Damasceno CMD, et al. Development and evaluation of stability of a gel formulation containing the monoterpene borneol. Sci World J. 2016;7394685.

59. Nasr M, Younes H, Abdel-Rashid RS. Formulation and evaluation of cubosomes containing colchicine for transdermal delivery. Drug Deliv Transl Res. 2020;10:1302–13.

60 Naseef H, Sahoury Y, Farraj M, Qurt M, AbukhalilAD, et al. Novel fusidic acid cream containing metal ions and natural products against multidrug-resistant bacteria. Pharmaceutics. 2022;14:1638.

61. El Shall AA, Ghoneim AM, Abdel-Mageed HM, et al. Ex vivo permeation parameters and skin deposition of melatonin-loaded microemulsion for treatment of alopecia. Futur J Pharm Sci. 2022;8:28.

62. Khan MI, Yaqoob S, Madni A, Akhtar MF, Sohail MF, et al. Development and in vitro/ex vivo evaluation of lecithin-based deformable transfersomes and transfersome-based gels for

combined dermal delivery of meloxicam and dexamethasone. BioMed Res Int. 2022. https://doi.org/10.1155/2022/8170318.

63. Liu CH, Huang HY. Antimicrobial activity of curcumin-loaded myristic acid microemulsions against Staphylococcus epidermidis. Chem Pharm Bull. 2012;60:1118–24.

64. Abdelhamed FM, Abdeltawab NF, ElRakaiby MT, Shamma RN, Moneib NA. Antibacterial and anti-inflammatory activities of thymus vulgaris essential oil nanoemulsion on acne vulgaris. Microorganisms. 2022;10:1874.

Publisher's Note Springer Nature remains neutral with regard to jurisdictional claims in published maps and institutional affiliations.